PAPER

NJC
www.rsc.org/njc

A highly efficient redox chromophore for simultaneous application in a photoelectrochemical dye sensitized solar cell and electrochromic devices

Ana F. Nogueira,*[a] Sérgio H. Toma,[b] Marcio Vidotti,[b] André L. B. Formiga,[b] Susana I. Córdoba de Torresi[b] and Henrique E. Toma*[b]

[a] *Instituto de Química, Universidade Estadual de Campinas, Caixa Postal 6154, Cep 13084-862 Campinas, SP, Brazil. E-mail: anaflavia@iqm.unicamp.br*
[b] *Instituto de Química, Universidade de São Paulo, Caixa Postal 26077, Cep 05513-970 São Paulo, SP, Brazil. E-mail: henetoma@iq.usp.br*

Received (in St. Louis, MO, USA) 21st July 2004, Accepted 6th October 2004
First published as an Advance Article on the web 5th January 2005

We synthesized a novel series of compounds based on a ruthenium(II) dicarboxybipyridine (dcbpy) complex containing chloro and *trans*-1,4-bis[2-(4-pyridyl)ethenyl]benzene (BPEB) ligands. The binuclear species $Na_6[\{[Ru^{II}(dcbpy)_2Cl\}_2(BPEB)]$ exhibits an electrochromic effect when reduced, which is assigned to the radical $BPEB^{0/\cdot}$, similarly as in viologen-based compounds. The carboxylate groups on the 4,4′ positions of bipyridine allow a strong attachment to the TiO_2 surface, contributing to an efficient and reversible electron transfer from the oxide to the chromophoric ligand, coloring the oxide film blue. The coloration efficiency CE(λ) at 633 nm was 109 cm^2 C^{-1}, which is high compared to TiO_2 itself. The complex also exhibits a high photon-to-electron conversion efficiency (IPCE > 70%) when applied as a photoanode in a dye sensitized solar cell (DSSC).

Introduction

Nanocrystalline semiconductor films have become widely used materials for many technological applications mainly due to their high surface-to-area ratio, light transparency, charge-separating properties and electronic conductivity. Modification of these wide-band-gap semiconductors by molecular compounds opens up an opportunity to explore the charge separation in the semiconductor interface in view of the development of new molecular devices. Semiconductor films, especially TiO_2, ZnO and SnO_2, are now very promising components in the development of dye sensitized solar cells,[1,2] electrochromic devices,[2–4] sensors, and (photo)electrocatalytic[5] and photochromic cells.[6–8]

The use of nanocrystalline electrodes in electrochromic devices, in which a monolayer of a redox chromophore is attached to the nanoparticle surface, allows an increase in the coloration of the films due to a high concentration of chromophores and fast switching times. Several redox molecules containing a surface anchoring group have been tested, including the well-established viologens,[2,9–11] and several metal complexes with different ligands.[12–16]

In this present work we prepared a novel compound based on a ruthenium(II) dicarboxybipyridine (dcbpy) complex containing chloro and *trans*-1,4-bis[2-(4-pyridyl)ethenyl]benzene (BPEB) ancillary ligands. This compound corresponds to the binuclear species $Na_6[\{Ru^{II}(dcbpy)_2Cl\}_2(BPEB)]$ (**1**). The ancillary BPEB ligand is a typically conjugated bridging ligand, which allows electron transport as well as intramolecular photoinduced electron-transfer or energy-transfer processes.[17] It also exhibits an electrochromic effect when reduced to the radical $BPEB^{0/\cdot}$, similarly as the viologen compounds.[18] Due to a very interesting spectroelectrochemical behavior when BPEB is combined with a ruthenium polypyridyl group, this complex has been intensively investigated, showing interesting electrochromic and photoelectrochemical phenomena when adsorbed onto TiO_2 films. The presence of carboxylate groups in the 4,4′ positions of bipyridine allows a strong attachment to the oxide surface, contributing to an efficient and reversible electron transfer from the oxide to the chromophoric ligand. This complex also exhibits a high photon-to-electron conversion efficiency when applied as sensitizer in dye sensitized solar cells. In order to gain more insight into the photoelectrochemical behavior of this complex, we have also investigated two analogous complexes containing bpy and BPEB as ligands, the mononuclear species $[Ru(bpy)_2Cl(BPEB)](PF_6)$ (**3**) and the binuclear one, $[\{Ru(bpy)_2Cl\}_2(BPEB)](PF_6)_2$ (**2**).[19] The structures of all compounds investigated are displayed in Fig. 1.

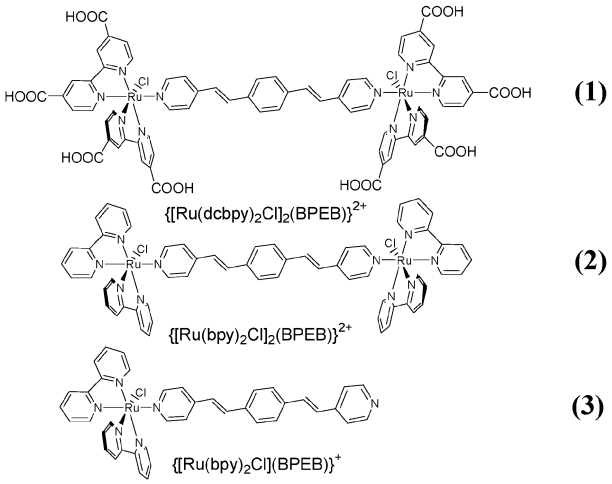

(1)

(2)

(3)

Fig. 1 Schematic representation of the molecular structure of the binuclear complexes $Na_6[\{Ru^{II}(dcbpy)_2Cl\}_2(BPEB)]$ (**1**) and $[\{Ru(bpy)_2Cl\}_2(BPEB)](PF_6)_2$ (**2**) and the mononuclear species $[Ru(bpy)_2Cl(BPEB)](PF_6)$ (**3**).

DOI: 10.1039/b411122b

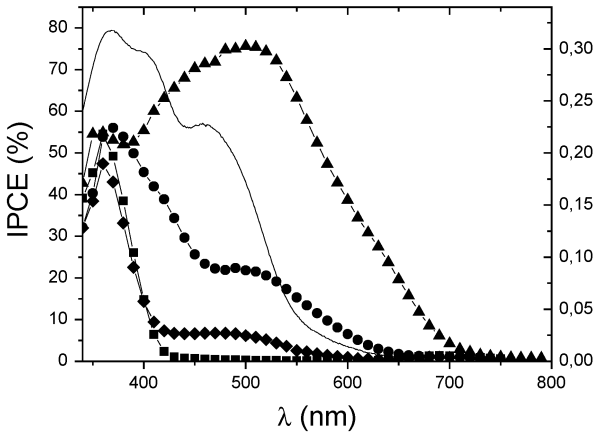

Fig. 2 Incident to Photon-to-Current Conversion Efficiency (IPCE) curves as a function of wavelength for the sensitizers: (–▲–) $[\{Ru^{II}(dcbpy)_2Cl\}_2(BPEB)]^{6-}$ (**1**); (–◆–) $[\{Ru(bpy)_2Cl\}_2(BPEB)]^{2+}$ (**2**) and (–●–) $[Ru(bpy)_2Cl(BPEB)]^{+}$ (**3**). For comparison we also show the curve for bare TiO_2 (–■–). The absorption spectrum of the binuclear species **1** in water solution is also shown (full line).

Results and discussion

For both photochemical and electrochemical experiments, a monolayer of the ruthenium complex was adsorbed onto a nanostructured TiO_2 film (4 μm thick) on a SnO_2:F^- electrode. This film acts as the working electrode in both arrangements. The active area was limited to 1 cm^2.

Photoelectrochemical response

Fig. 2 shows the complex absorption spectrum of the binuclear species **1** together with the incident photon-to-current conversion efficiency (IPCE) curves as function of wavelength for all sensitizers. The UV bands in the electronic spectrum are attributed to the ligand-centered (LC) transitions, while the two visible bands are attributed to metal-to-ligand charge transfer: $Ru^{II}(d\pi) \rightarrow BPEB(p\pi^*)$ ($MLCT_1$) at 400 nm and $Ru^{II}(d\pi) \rightarrow dcbpy(p\pi^*)$ ($MLCT_2$) at 458 nm.[19]

The IPCE curve as a function of wavelength for the species **1** extends further into the infrared region and resembles the ruthenium complex absorption spectrum, exhibiting a broad band from 420–530 with a peak centered at 500 nm with a maximum of 75%. These values are comparable to the well-known Ru^{II} polypyridyl complex containing SCN^- (N3)[1] and other analogous complexes.[20–22]

The contribution of both charge transfer transitions to the photocurrent spectra is noteworthy. Such a high efficiency cannot be explained in terms of the π donor-acceptor properties of the ancillary ligand, as BPEB is more characterized as a π-acceptor.[23] Another interesting point is the red-shift of both MLCT transitions in comparison with the spectrum in solution. The $MLCT_2$ red-shift is straightforward because the complex is strongly bound to the TiO_2 surface *via* the carboxylate groups. The red-shift observed for the $MLCT_1$ band is quite surprising and can only be explained if there is a strong mixing between the BPEB and bpy ligands. Theoretical calculations were performed in order to address the nature of this coupling and will be discussed below.

Table 1 Molecular orbital energy order and fractional orbital mixing of $[\{Ru(dcbpy)_2Cl\}_2(BPEB)]^{6-}$

Molecular orbital	Energy/eV	% Fractional orbital mixing				
		Ru^{II}	Cl^-	BPEP	CO_2^-	Bpy
252	6.72	6.66	0.32	9.52	1.96	81.54
251	6.55	5.16	0.21	5.47	2.06	87.10
250	6.51	3.78	0.10	5.45	2.07	88.59
249	6.06	1.75	0.04	83.10	0.37	14.74
248 (LUMO)	**5.53**	**2.72**	**0.04**	**92.91**	**0.11**	**4.22**
247 (HOMO)	**1.03**	**60.91**	**1.37**	**13.00**	**1.44**	**23.29**
246	0.99	61.40	1.60	11.44	1.53	24.04
245	0.71	71.61	3.33	3.56	1.30	20.20
244	0.70	71.86	3.24	3.77	1.27	19.86
243	0.56	77.45	4.67	0.98	0.82	16.08

The other species containing a non-carboxylate bpy ligand exhibited a much lower IPCE in comparison to species **1**. Surprisingly, the mononuclear specie **3** presents IPCE values reaching 50% around 400 nm and another broad peak centered at 500 nm, corresponding to 20% of monochromatic efficiency. Although this species does not possess any strong binding group, the presence of a free pyridyl group on the BPEB ligand can be responsible for its attachment to the TiO_2 surface, as was previously observed for several tetrapyridylporphyrins.[24] The binuclear species **2**, however, displayed almost no photocurrent due to the lack of an anchoring group. For comparison, the efficiency of bare TiO_2 is also shown.

In order to understand the electronic effects involved in photocurrent generation, Lever and Grätzel[25] employed ZINDO/S calculations and demonstrated the importance of ruthenium 4d and ligand π* orbital mixing. Such a delocalization is also observed in compound **1**. We also performed molecular modelling using PM3/ZINDOS applied to the binuclear species **1**. The relevant HOMO and LUMO levels and the fractional orbital mixture are shown in Table 1 while the theoretical and experimental electronic spectra are collected in Table 2.

Our modelling shows that the HOMO level involves a mixture of orbitals from ruthenium, bpy and BPEB while the LUMO level is predominantly centered on the BPEB ligand with a minor contribution from half of the dcbpy ligands (Fig. 3). The theoretical spectrum agrees very well with the experimental one and the nature of the absorption bands could be assigned unambiguously. The important transitions that contribute to photocurrent generation are real MLCT to both ligands: the well-known $Ru^{II}(d\pi) \rightarrow dcbpy(p\pi^*)$ CT and a low-energy shoulder $Ru^{II}(d\pi) \rightarrow BPEB(p\pi^*)$ CT. Thus, upon excitation, both ruthenium centers populate LUMO levels composed of both bpy and BPEB ligands; this is responsible for electron injection into the TiO_2 conduction band.

Table 2 Selected theoretical electronic transitions of $[\{Ru(dcbpy)_2Cl\}_2(BPEB)]^{6-}$

Observed λ/nm	Theoretical λ/nm	Assignment $MO_i \rightarrow MO_f$	
590 sh[a]	629.6 (0.72)[b]	247 → 248; 246 → 249	Ru → BPEB CT
	598.1 (0.55)	245 → 248; 244 → 249	*ibidem*
	584.3 (0.11)	243 → 248; 242 → 249	*ibidem*
458	514.5 (0.31)	243 → 251; 242 → 250	Ru → bpy CT
	385.8 (0.20)	247 → 257; 246 → 256	*ibidem*
400	368.4 (0.08)	247 → 261; 246 → 260	Ru → BPEB|bpy (50%|50%) CT
	360.1 (0.06)	247 → 249; 246 → 248	Ru → BPEB CT

[a] sh = shoulder. [b] Oscillator strength is given in parentheses.

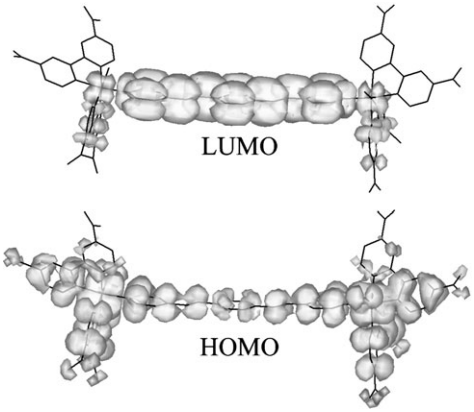

Fig. 3 Probability density functions of HOMO and LUMO levels of the complex **1**.

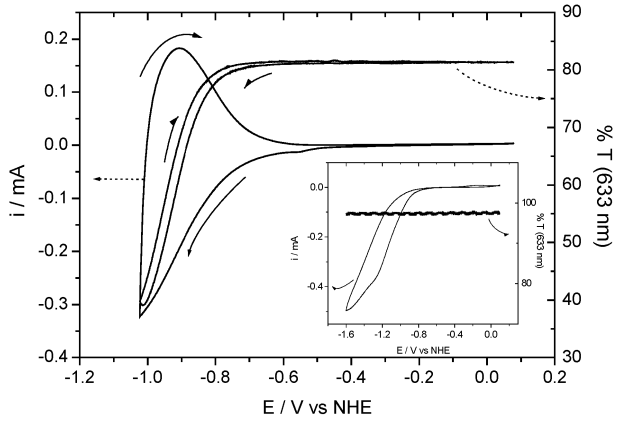

Fig. 4 Cyclic voltammetry of a nanocrystalline TiO_2 film modified with the chromophore $[\{Ru^{II}(dcbpy)_2Cl\}_2(BPEB)]^{6-}$. The graphic also shows the change of transmittance measured simultaneously at 633 nm. The inset shows the behavior of pristine TiO_2 under the same conditions. Solution: DMF/$LiClO_4$, $v = 5$ mV s^{-1}, Pt foil as counter-electrode.

The current-voltage data for the photoelectrochemical cells sensitized with the species **1–3** (100 mW cm^{-2} irradiation using a Xenon lamp) are summarized in Table 3. As expected the best results were obtained with the TiO_2 cell sensitized with complex **1**.

Spectroelectrochemical investigation

For the electrochemical experiments, we employed 0.2 M $LiClO_4$ in dry DMF as electrolyte. Due to hydrogen evolution over potential, it was not possible to determine the complex reduction potential in water. However, its analogous binuclear complex $[\{Ru^{II}(bpy)_2Cl\}_2(BPEB)](PF_6)_2$ (**2**) shows BPEB first and second reduction waves at −0.97 ($BPEB^{1-/0}$) and −1.15 ($BPEB^{2-/1-}$) V *vs.* NHE .[19] Assuming that for the carboxylic binuclear complex the reduction waves will not differ substantially and that the presence of Li^+ in the aprotic DMF solvent shifts the TiO_2 flat band potential positively to −0.2 to −0.4 V, we can conclude that the reduction potential of the anchored complex lies above the conduction band edge of TiO_2 at the liquid–solid interface. This situation allows for electrons to be transferred reversibly from the conduction band to the molecule and the semiconductor becomes conducting for the adsorbed species. We have previously studied the electrochromic behavior of the BPEB ligand alone and complexed to $[Ru^{II}(bpy)_2Cl]_2$, which resembles that of the viologen compounds. The first reduction generates the radical ($BPEB^{1-/0}$), which has two strong near infrared bands centered at 718 and 781 nm, turning the electrode blue. These bands correspond to the $\pi \rightarrow \pi^*$ transition in the radical cation. The second reduction gives rise to $BPEB^{2-/1-}$ species, which are almost colorless, showing also the disappearance of the infrared bands.

In order to elucidate the spectroelectrochemical behavior of the binuclear complex $[\{Ru^{II}(dcbpy)_2Cl\}_2(BPEB)]^{6-}$ adsorbed onto a TiO_2 transparent film, cyclic voltammograms (CVs) were measured for both the modified and pristine TiO_2 films. Fig. 4 shows the CVs accompanied by measurements of the optical absorption changes at 633 nm, for the modified electrode $TiO_2/[\{Ru^{II}(dcbpy)_2Cl\}_2(BPEB)]\}^{6-}$ and for the pristine TiO_2.

No color change due to Li^+ intercalation was detected for the pristine TiO_2 films up to −1.6 V *vs.* NHE; the electrochemical response is probably due to solvent degradation. On the basis of the CV shown on Fig. 4, we observe that the complex molecules chemisorbed on the nanostructured TiO_2 electrode undergo a single electron reduction from −0.7 V to −1.0 V *vs.* NHE. This reduction process corresponds to the formation of the radical anion in the BPEB ligand, coloring the electrode blue. This reduction process is accompanied by a change of 42% in the film transmittance, from almost transparent to deep blue colored. Both electrochemical and optical changes were shown to be stable up to this potential and the electrode color change was completely recovered after oxidation-reduction processes, showing that the electrochromic conversion is highly reversible. The coloration efficiency CE(λ) at 633 nm, defined by eqn. (1):

$$CE(\lambda) = \frac{\Delta A(\lambda)}{\Delta Q} \qquad (1)$$

in terms of absorbance changes (ΔA) and charge involved (ΔQ), is 109 cm^2 C^{-1}, which is high compared with TiO_2 itself (8 cm^2 C^{-1} at 633 nm) and to other electrochromic transition metal oxides cited in the literature, like NiO_x (40 cm^2 C^{-1}), CoO_x (50 cm^2 C^{-1}) and close to WO_3 (70–100 cm^2 C^{-1}).[26] Below −1.0 V *vs.* NHE, we would expect a second reduction of the radical cation BPEB. However, due to the closeness of both BPEB reduction processes, the second reduction wave was not detected for the complex adsorbed onto the oxide surface.

Table 3 *I-V* data of the TiO_2 photoelectrochemical cells sensitized by the complexes $Na_6[\{Ru^{II}(dcbpy)_2Cl\}_2(BPEB)]$ (**1**), $[\{Ru(bpy)_2Cl\}_2(BPEB)](PF_6)_2$ (**2**) and $[Ru(bpy)_2Cl(BPEB)](PF_6)$ (**3**)

Complex	I_{sc}/mA cm^{-2}	V_{oc}/V	FF
1	3.2	0.680	0.53
2	0.32	0.458	0.52
3	1.16	0.567	0.44

Conclusion

In summary, the exceptional electrochromic behavior and the high photon-to-current conversion efficiency exhibited by the chromophore $[\{Ru^{II}(dcbpy)_2Cl\}_2(BPEB)]^{6-}$ open up several possibilities of future applications in electrochromic windows and dye sensitized photoelectrochemical cells. The simultaneous electrochromic and photoelectrochemical properties make the use of this dye most suitable for applications in self-powered electrochromic windows, in which a DSSC can provide the power required to switch on the device.[27]

Experimental

General

All solvents and reactants were of analytical grade and employed without further purification. The starting $[Ru(dcbpy)_2Cl_2]$ compound was obtained based on a classical method reported in the literature.[28] *trans*-1,4-Bis[2-(4-pyridyl)ethenyl]-benzene (BPEB) was prepared by the Heck method[29,30] and

purified by recrystallization from a hot ethanol–water mixture. Anal. found: C, 83.4%; H, 5.8%; N, 9.7%; required for $C_{20}H_{16}N_2$ (MW = 284.36 g mol^{-1}): C, 84.5%; H, 5.7%; N, 9.6%. MS: *m/z* 285.12 $[M + H]^+$. The compounds $[Ru(bpy)_2Cl(BPEB)](PF_6)$ (**3**) and $[\{Ru(bpy)_2Cl\}_2(BPEB)](PF_6)_2$ (**2**) were prepared according to a previous report.[19]

The UV-Vis spectra were obtained with a HP-8453A diode array spectrophotometer in distilled water solution.

Synthesis of $Na_6[\{Ru(dcbpy)_2Cl\}_2(BPEB)]$ (1)

The $Na_6[\{Ru(dcbpy)_2Cl\}_2(BPEB)]$ complex was prepared by modification of a previous method described in the literature.[19] $[Ru(dcbpy)_2Cl_2]$ (200 mg; 0.3 mmol) and BPEB (28.4 mg; 0.1 mmol) were added to 110 ml of a 5 : 1 MeOH–H_2O solvent mixture and heated at reflux under argon atmosphere. After 2 h refluxing, a brown precipitate was formed. The mixture was allowed to cool and concentrated to *ca.* 50 ml by rotary evaporation. The resulting precipitate was separated from solution by vacuum filtration, washed with few portions of cold MeOH and diethyl ether, and dried under vacuum (yield = 55%). In order to increase the solubility of the complex, a few drops of NaOH (pH = 10) solution were added to the compound, converting it to a sodium salt. Anal. found: C 50.91%, H 3.4% and N 8.7%; required for $C_{68}H_{46}N_{10}O_{16}Cl_2Ru_2 \cdot 4H_2O$: C 50.96%, H 3.7% and N 8.6%.

Preparation of nanoporous TiO_2 films

The nanoporous TiO_2 film for photoelectrochemical measurements, which was deposited onto a sheet of F-doped SnO_2 TEC15 conducting glass (sheet resistance $\sim$15 Ω cm^{-2}), was prepared using a variation of a previously published procedure.[1] A colloidal TiO_2 suspension was obtained by grinding 6 g of TiO_2 powder in 2 ml of distilled H_2O and 0.2 ml of acetylacetone, in a mortar with a pestle, for about 40 min. Finally 8.0 ml of distilled water and 0.1 ml of Triton X-100 were slowly added with continuous mixing for 10 min.

A previously cleaned conductive glass sheet was laid on a flat surface with the conductive side up and the deposition area was delimited with plastic adhesive tape. Several drops of the above TiO_2 suspension were spread as evenly as possible onto the surface using a glass rod. The thickness of the TiO_2 coating ($\sim$4 μm) was determined by the thickness of the adhesive tape. The electrodes were then dried in air and fired in a furnace, at 450 °C for 30 min.

For the preparation of the transparent TiO_2 films, colloidal TiO_2 paste purchased from Solaronix was kindly provided by Prof. De Paoli.

Surface treatment with dye

The electrodes covered by a nanoporous TiO_2 film layer were immersed overnight in a 1.0×10^{-4} M solution of the complex $Na_6[\{Ru(dcbpy)_2Cl\}_2(BPEB)]$ in distilled water to achieve the adsorption equilibrium condition. After overnight immersion, the electrodes were washed with ethanol and dried in moisture-free air. It is important to point out that in the carboxylic form the binuclear complex is very poorly soluble in water. However, in the carboxylate form the solubility increases considerably. The TiO_2 surface coverage could be observed by the change in transmittance measured at 633 nm in the electrochemical experiments comparing to the bare TiO_2 film as shown in Fig. 4. For the electrochromic measurements, after washing the electrodes with ethanol, they were kept in a vacuum and protected from light for 8 h prior to assembling the cell.

The optical density of the film and the color change, from white to the color of the attached dye. Afterward overnight immersion, the electrodes were washed with ethanol and dried in moisture-free air. For the electrochromic measurements, after washing the electrodes with ethanol, they were kept in vacuum and protected from light for 8 h prior to assembling the cell.

Assembling the DSSC cell

The cell (1.0 cm^2 active area) was assembled by transferring about 1 ml of the electrolyte solution (0.5 M *t*-butylpyridine, 0.6 M tetrabutylammonium iodide, 0.1 M LiI, 0.1 M I_2 in 10 ml methoxyproprionitrile) onto the SnO_2:F^- glass covered with TiO_2/attached dye. The counter electrode was then pressed against the TiO_2/dye film. The transparent counter electrode was treated by transferring a drop of 0.05 mol l^{-1} solution of H_2PtCl_6 in isopropanol onto the conducting glass and firing at 420 °C in air for 20 min. A PVC film was placed in-between the two electrodes to avoid short circuits and electrolyte leakage. A clamp kept the assembly together. No further sealing was necessary, at least for the tests described in this communication.

Measurement of the photoelectrochemical properties

The DSSC photoelectrochemical cells were firmly placed in an optical bench for the characterization procedures. The IPCE spectra and the current-voltage (*I-V*) curve were obtained using an Applied Photophysics 150 W Xenon lamp as a white-light source and a home-made resistor as a variable load. An Oriel Spectral Luminator was employed as the monochromatic source. The light intensity was varied from 1 to 2 mW cm^{-2}. Measurements of photocurrent and photovoltage were performed using an Autolab Eco Chimie PGSTAT 30 potentiostat and a Count Digital Multimeter HC 608. The sample was always illuminated through the conducting glass substrate and no corrections were made for the 30% reflection and transmission losses in the SnO_2:F^- glass. The poly- and monochromatic light intensity at the electrode position were measured with a Newport Optical Power Meter model 1830-C.

Measurement of the electrochromic properties

The electrochemical measurements were carried out in a 0.2 M $LiClO_4$ solution of dry dimethylformamide (DMF) by using a potentiostat/galvanostat from Ecochemie, model AUTOLAB PGSTAT 30. A conventional three-electrode cell consisting of a platinum foil counter electrode and a silver wire as pseudo reference electrode (+100 mV *vs.* NHE) was employed. Chromogenic analysis was made simultaneously with voltammetric experiments using a solid-state light source (WPI, Inc.). Plastic fiber optic cables up to 1 mm in diameter were used to deliver light from the cell to a PDA 1 photodiode amplifier (WPI, Inc.), designed for low light level detection with a current resolution of typically 1 pA. The output signal of the PDA 1 was delivered to the analogical input of the potentiostat and both current and transmittance were collected simultaneously.

Theoretical calculations

Molecular modelling calculations were carried out for the $[\{Ru(dcbpy)_2Cl\}_2(BPEB)]^{6-}$ complex, starting with the PM3[31] implementation of the HyperChem program[32] for geometry optimization, and using a gradient of 1×10^{-5} kcal $Å^{-1}$ mol^{-1} as a convergence criterion in a conjugated gradient method. SCF molecular orbital calculations were performed at the RHF level, using the ZINDO/S method[33] and the default parameters (and scaling factors $k_{p\sigma} = 1.267$ and $k_{p\pi} = 0.585$). The electronic spectrum was calculated, based on single CI excitations in an active space involving 60 frontier molecular orbitals (40 highest occupied and 20 lowest unoccupied MOs).

Acknowledgements

We thank L. F. O. Furtado for helping with the collection of the experimental data, as well as M.-A. De Paoli and Degussa for providing the TiO_2 powder and paste, respectively. We also thank CNPq (CT-ENERG/CNPq-Proc. 400804/2003-4), FAPESP, RENAMI and Instituto do Milênio de Materiais Complexos for the financial support.

References

1 M. K. Nazeeruddin, A. Kay, R. Humphry-Baker, E. Muller, P. Liska, N. Vanchopoulos and M. Grätzel, *J. Am. Chem. Soc.*, 1993, **115**, 6382.
2 K. Kalyanasundaram and M. Grätzel, *Coord. Chem. Rev.*, 1998, **77**, 347.
3 X. Marguerettaz, R. O'Neill and D. Fitzmaurice, *J. Am. Chem. Soc.*, 1994, **116**, 2629.
4 R. Cinnsealach, G. Boschloo, S. N. Rao and D. Fitzmaurice, *Sol. Energy Mater. Sol. Cells*, 1998, **55**, 215.
5 B. O'Reagan and M. Grätzel, *Nature (London)*, 1991, **353**, 737.
6 C. Bechinger, S. Ferrer, A. Zaban, J. Sprague and B. A. Gregg, *Nature (London)*, 1996, **383**, 608.
7 P. Bonhote, J. E. Moser, N. Vlachopoulos, L. Walder, S. M. Zakeeruddin, R. HumphryBaker, P. Pechy and M. Grätzel, *Chem. Commun.*, 1996, **10**, 1163.
8 K. Naoi, Y. Ohko and T. Tatsuma, *J. Am. Chem. Soc.*, 2004, **126**, 3664.
9 F. Campus, P. Bonhôte, M. Grätzel, S. Heinen and L. Walder, *Sol. Energy Mater. Sol. Cells*, 1999, **56**, 281.
10 P. Bonhôte, J. E. Moser, N. Vlachopoulos, L. Walder, S. M. Zakeeruddin, R. Humphry-Baker, P. Pechy and M. Grätzel, *J. Am. Chem. Soc.*, 1999, **121**, 1324.
11 D. Cummins, G. Boschloo, M. Ryan, D. Corr, R. Nagaraja and D. Fitzmaurice, *J. Phys. Chem. B*, 2000, **104**, 11449.
12 J. Garcia-Cañadas, F. Fabregat-Santiago, J. Kapla, J. Bisquert, G. G. Belmonte, I. Mora-Seró and M. O. M. Edwards, *Electrochim. Acta*, 2004, **49**, 745.
13 F. Pichot, J. H. Beck and C. M. Elliot, *J. Phys. Chem. A*, 1999, **103**, 6263.
14 J. García-Cañadas, A. P. Meacham, L. M. Peter and M. D. Ward, *Electrochem. Commun.*, 2003, **5**, 416.
15 M. Biancardo, P. F. H. Schwab, R. Argazzi and C. A. Bignozzi, *Inorg. Chem. Commun.*, 2003, **42**, 3966.
16 P. F. H. Schwab, S. Diegoli, M. Biancardo and C. A. Bignozzi, *Inorg. Chem. Commun.*, 2003, **42**, 6613.
17 M. D. Ward, *Chem. Soc. Rev.*, 1995, 121.
18 W. D. Bates, P. Chen, C. A. Bignozzi, J. R. Schoonover and T. J. Meyer, *Inorg. Chem.*, 1995, **34**, 6215.
19 S. H. Toma, M. Uemi, S. Nikolaou, D. M. Tomazela, M. N. Eberlin and H. E. Toma, *Inorg. Chem.*, 2004, **43**, 3521.
20 K. Kalyanasundaram and M. Grätzel, *Coord. Chem. Rev.*, 1998, **77**, 347.
21 R. Argazzi, C. A. Bignozzi, T. A. Heimer, F. Castellano and G. J. Meyer, *Inorg. Chem.*, 1994, **33**, 5741.
22 O. Kohle, S. Ruile and M. Grätzel, *Inorg. Chem.*, 1996, **35**, 4779.
23 C. A. Bignozzi, R. Argazzi and C. Kleverlaan, *Chem. Soc. Rev.*, 2000, **29**, 87.
24 A. F. Nogueira, A. L. B. Formiga, H. Winnischofer, M. Nakamura, F. M. Engelmann, K. Araki and H. E. Toma, *Photochem. Photobiol. Sci.*, 2004, **3**, 56.
25 (*a*) M. K. Nazeeruddin, S. M. Zakeeruddin, R. Humphry-Baker, S. I. Gorelsky, A. B. P. Lever and M. Grätzel, *Coord. Chem. Rev.*, 2000, **208**, 213; (*b*) T. Renouard, R.-A. Fallahpour, M. K. Nazeeruddin, R. Humphry-Baker, S. I. Gorelsky, A. B. P. Lever and M. Grätzel, *Inorg. Chem.*, 2002, **41**, 367.
26 (*a*) S. C. Oliveira, R. M. Torresi and S. I. Córdoba de Torresi, *Quim. Nova*, 2000, **23**, 79; (*b*) A. Surca, B. Orel, B. Pihlar and P. Bukovec, *J. Electroanal. Chem.*, 1996, **408**, 83; (*c*) C. G. Granqvist, *Handbook of Inorganic Electrochromic Materials*, Elsevier, Oxford, 1995; (*d*) S. I. Córdoba de Torresi, A. Gorenstein, R. Torresi and M. V. Vásquez, *J. Electroanal. Chem.*, 1991, **318**, 131; (*e*) C. N. Polo da Fonseca, Marco.-A. De Paoli and A. Gorenstein, *Sol. Energy Mater. Sol. Cells*, 1994, **33**, 73.
27 C. Bechinger and B. A. Gregg, *Sol. Energy Mater. Sol. Cells*, 1998, **54**, 405.
28 P. Liska, N. Vlachopoulos, M. K. Nazeeruddin, P. Comte and M. Gratzel, *J. Am. Chem. Soc.*, 1988, **110**, 3686.
29 R. F. Heck, *Org. React.*, 1981, **27**, 345.
30 A. J. Amoroso, A. M. W. C. Thompson, J. P. Maher, J. A. McCleverty and M. D. Ward, *Inorg. Chem.*, 1995, **34**, 4828.
31 (*a*) J. J. P. Stewart, *J. Comput. Chem.*, 1989, **10**, 209; (*b*) J. J. P. Stewart, *J. Comput. Chem.*, 1989, **10**, 221.
32 *HyperChem*, version 6.01 for Windows, Hypercube, Inc., Gainesville, FL, USA, 2000.
33 (*a*) M. C. Zerner, G. H. Loew, R. F. Kirchner and U. T. Mueller-Westerhoff, *J. Am. Chem. Soc.*, 1980, **102**, 589; (*b*) A. D. Bacon and M. C. Zerner, *Theor. Chim. Acta*, 1979, **53**, 21; (*c*) N. L. Ridley and M. C. Zerner, *Theor. Chim. Acta*, 1976, **42**, 223; (*d*) N. L. Ridley and M. C. Zerner, *Theor. Chim. Acta*, 1973, **32**, 111.